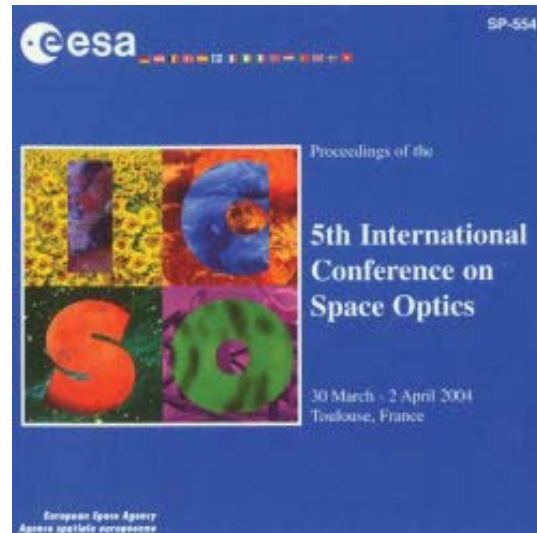


International Conference on Space Optics—ICSO 2004

Toulouse, France

30 March–2 April 2004

Edited by Josiane Costeraste and Errico Armandillo



Design and evaluation of ALMA band 9 quasioptical system

A. Baryshev, M. Carter, W. Jellema, R. Hesper



DESIGN AND EVALUATION OF ALMA BAND 9 QUASIOPTICAL SYSTEM

A. Baryshev^(1,3), M. Carter⁽²⁾, W. Jellema⁽¹⁾, R. Hesper^(1,3)

⁽¹⁾ SRON, Landleven 12, P.O.Box 800, 9700 AV, The Netherlands, E-mail:andrey@sron.rug.nl

⁽²⁾ IRAM, 300 Rue de la Piscine, Domaine de Universitaire de Grenoble, 38406, St. Martin d'Herès, France, E-mail: carter@iram.fr

⁽³⁾ Kapteyn Institute, RuG, Landleven 12, P.O. Box 800, 9700 AV Groningen, The Netherlands

ABSTRACT

The Atacama Large Millimeter Array (ALMA) project requires the development of reliable quasi-optical systems with requirements similar to the ones in space. The operating condition for optical elements of higher frequency channels are similar to the conditions in spacecraft, since these elements are contained within the ALMA cryostat in high vacuum and at cryogenic temperatures. The remote terrain of the Atacama Desert and the scale of project suggest that a significant effort should be made to ensure high reliability of the system. Therefore the techniques, common to a space mission are applied with this development.

In this report we would like to present the design of the quasi-optical system for ALMA band 9 (600-702 GHz) containing elements typical to a space system. A design assumptions and details will be presented for a frequency independent system. A measurement of near field antenna beam pattern (phase and amplitude) will be presented and comparison with theoretical predictions will be made.

1. INTRODUCTION

1.1 ALMA instrument

The Atacama Large Millimeter Array (ALMA) is an interferometric array of 64 heterodyne receivers. It is located at high altitude of 5000 meters in the northern Chile. This array is being built in collaboration between North America and Europe (represented by European Southern Observatory) with a possibility of Japan joining the project at a later stage.

Each antenna consists of a 12 m diameter parabolic main reflector, 0.75m diameter secondary mirror and a 10 band receiver. The receiver frequency coverage is 30-950GHz. It is subdivided into ten bands, corresponding to the regions of high atmospheric transmission. For the first scientific operations four frequency bands were chosen: 3(85 –116GHz), 6(211-275GHz), 7(275-375GHz) and 9(600-702GHz). All of these receivers are dual polarization and have sideband

separation or double sideband Superconductor – Isolator – Superconductor (SIS) tunnel junction mixers. A wide Intermediate Frequency (IF) bandwidth of 8GHz was chosen as a baseline requirement.

The chosen mixer technology requires cryogenic temperatures of liquid Helium level (4K) and high vacuum. These conditions are very close to one in space. High number of systems to be produced is also required, thus a special attention should be paid to a product/quality assurance [1,2,3].

1.2 ALMA front-end design

The artist impression of ALMA front-end cryostat is shown in fig. 1. Each front-end holds 10 subsystems called cartridges and provides three temperature levels to each structure: 4K, 12K, 90K and ambient temperature.

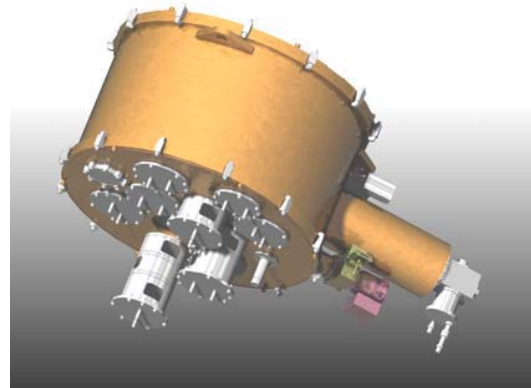
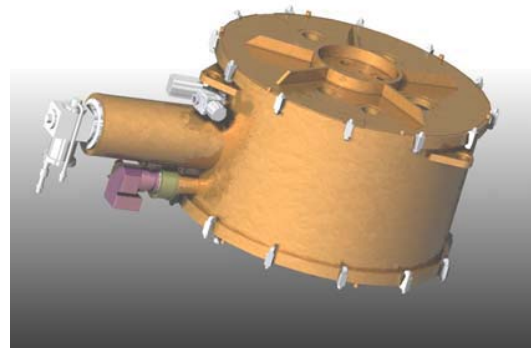


Fig. 1 An artist impression of ALMA front-end cryostat holding 10 cartridge subsystems. Design is done by Rutherford Appleton Laboratory (UK).



Fig. 2 Photograph of band 9 cartridge structure. Design is made by Rutherford Appleton Laboratory (UK).

A specially designed flexible links allow for insertion of cartridges from the bottom of front-end cryostat without accessing an internal structure to provide a heat link [5].

All cartridges are mounted from the bottom of cryostat. The internal cryogenic connections are made automatically during cool down. This concept allows a significant reduction to maintenance time, since the Dewar does not need to be disassembled for cartridge changes.

The telescope beam is entering the cryostat from the top with the telescope beam waist located near the cryostat optics windows. Lower frequency bands have active optical elements (lenses and elliptical mirrors) mounted outside the cryostat vacuum space. For frequency bands 5 – 10 all optics are contained within the cartridge at 4K.

The cartridge structure, which all receiver elements per frequency band will be mounted, is presented in fig. 2. The Sumimoto refrigerator, which cools the cryostat, provides four temperature levels (4K, 12K, 90K and ambient). Each cartridge stage is cooled by clamping with its flexible heat links. The mechanical reference for 4 K plate is provided via cartridge support structure from ambient temperature mount. A finite element analysis was performed to ensure that cartridge structure is rigid enough to perform within tolerance for all telescope elevation angles (from 0° to 90°).

2. BAND 9 OPTICS DESIGN

2.1 Design requirements and concept

The band 9 receiver optics has the following main design goals: a) all optics is mounted in the cartridge structure shown in fig. 2; b) the LO power source is located on the 90 K stage of the cartridge; c) most of the optics is located at 4 K level since SIS mixer technology is used; d) two orthogonal linear polarizations should be received from the sky; e) the secondary mirror edge illumination taper should be 12 dB and should not depend on frequency within ALMA band 9.; f) design should be based on the reflective optics elements and five waists size beam should be put through; g) Cross polarization signal level should be less than -20 dB from the power in the main polarization.

ALMA antenna is a classical Cassegrain system. The primary mirror diameter is about 12 m, secondary mirror diameter is 0.75 m, and the distance from antenna secondary mirror to focus is 6 m. Antenna beam towards receiver is #f8 angular size. This is an input beam for band 9 receiver. The receiver position is 0.1 m offset from main symmetry axis of antenna.

Additional attention should be paid to the small series production of the optics. ALMA project requires 64 receivers to be built. Because of this requirement it was decided to build all the optics using conventional CNC machining and make machining tolerances sufficiently tight to skip the additional alignment procedure by a laser beam.

Since the frequency with band 9 is much lower than that of optical light only 7 micron RMS mirror roughness is required, and the tightest tolerance for this particular design is about 40 microns. These parameters are well within reach of conventional CNC machining techniques. Note that 7 micron RMS will not allow the optical checks for mirror alignment and therefore use of an submm wave antenna beam pattern measurement system is essential to assess the quality of optical system. In order to verify the design concept of using direct CNC machining for these frequencies, a simple model for a signal chain – a two-mirror block has been built, together with a mixer horn, the details of it will be presented later in the section about measurement results.

2.2 Signal path

Drawing of signal path is presented in fig.~3. Telescope focus is located in the point FP. Two elliptical mirrors (M3, M4) are used to reimagine the secondary mirror of telescope (M2) into the mouth of a mixer horn with the size, that is appropriate for 12 dB edge taper. The quarterly focal point (the second focal point of mirror M4) coincides with an apex of the corrugated horn H1. This construction allows for

frequency independent coupling of the telescope beam to a corrugated horn feed. Mirror diameters are chosen to put through a 5 w size beam.

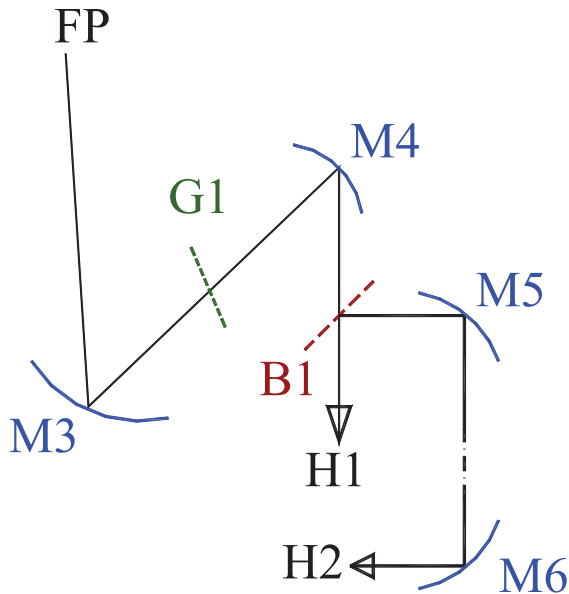


Fig. 3 Layout of optics. Beam dumps and one of the signal polarizations are not shown.

The second polarization beam is split off from the main beam at 90 degrees angle by means of a grid G1. The grid is located between mirrors M3 and M4 at the narrowest point of the beam (near tertiary focus). M3 is used for both polarizations and additional mirrors M4', M5', and M6' are used for forming an orthogonal polarization beam arriving at second mixer horn H2. The cross polarization signals are absorbed by a special absorber plate mounted behind the grid G1 at 4K level.

2.3 LO insertion

Local oscillator signal is inserted quasioptically using a beamsplitter B1 in fig. 3. It is mounted between signal horn and mirror M4. A 12 micron Mylar film is used as beamsplitter material that corresponds to approximately 7% of LO signal insertion. The LO signal is then reflected towards 90 K plate of the cartridge where additional mirror M6 and final local oscillator multiplier (quintupler) is located. The quintupler beam is formed by a horn H2. The system is designed to put through a four waists size beam. Additional infrared heat filters are mounted on 12 K stage to decouple 4K and 90 K levels thermally.

The second polarization has its LO inserted in exactly the same way using mirrors M5' and M6' that are identical to M5 and M6 respectively. It has its own multiplier and horn H2'. This polarization is not shown in fig. 3.

An absorber plate is mounted behind each of beamsplitters for both polarizations to dump LO power that is not coupled into the beam.

2.4 Opto-mechanical design

The layout that is briefly described below has to be realized in practice, i.e. mirrors, beamsplitters, grids and mixer horns have to be mounted within a certain tolerances with respect to each other and optics should be aligned. A tolerance budget was made for current optics layout indicating that 40 micron displacement is the highest requirement for displacement to produce 1% of efficiency loss [3,4].

The main idea of the design is to make all the parts in using CNC machining techniques observing tolerances. In this way all optics will be aligned upon assembly and no additional measures, like shimming or putting a laser beam through are not required. This allows for significant easing of requirements for mirror accuracy, grid foil flatness and beamsplitter flatness.

For example, as it can be seen from layout, mirrors M4, M5 and M4', M5' are pointing downwards. It is the most natural to make them out of one block in one CNC machining run. All beamsplitters and grids can be mounted in the block, also containing a mirror M3, which is directly machined in it. This concept is presented in fig. 4. The two blocks, bottom and top are bolted to each other within the required tolerances.

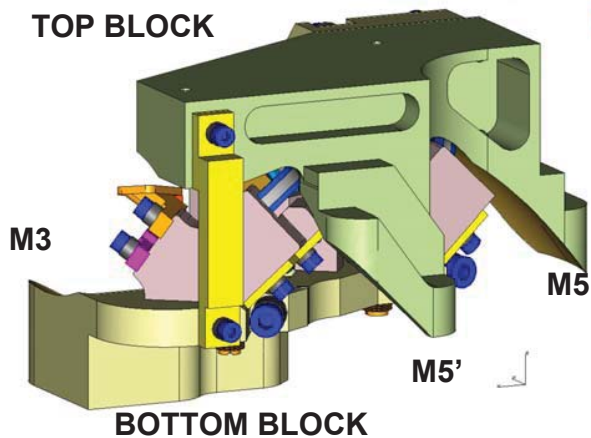


Fig. 4. Main signal optics design concept.

2.5 Prototype mirror block

In order to verify if a selected machining techniques or design approach works a simplified model of a signal path consisting of two mirrors M3, M4 and mixer horn mount has been built. It is shown in fig. 5

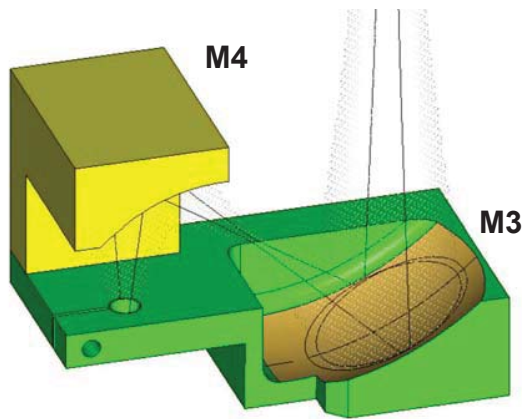


Fig. 5 A prototype two-mirror block for evaluating production techniques.

3. MEASUREMENT SYSTEM

3.1 Scanning system and detection technique

A Measurement System: The measurements were made in the near field of the optics under test and similar to that described in [6]. A small probe, which was the transmitter in front of the receiver in the X, Y and Z planes. These movements were made in small discrete steps and at each point values of amplitude and phase were taken. The transmitter was a phase locked Gunn oscillator working between 100-120 GHz, which fed a X6 multiplication chain to have a transmitted signal between 600 and 720GHz. A small part of the Gunn signal was coupled off to act as a reference for the phase. The signal was received through the optics under test with a harmonic mixer. A frequency about 20GHz was used from a synthesiser to mix both the reference and received signals so there was an IF of 4GHz and 4/6GHz respectively. The reference channel was multiplied by 6 so that 2 coherent signals of 4 GHz can be fed into a vector voltmeter, which gives the phase and amplitude information. This system is essentially a homodyne system.

For most of the measurements a network analyzer with an access to internal reference and signal ports was used. This allows for using very small detection bandwidths up to 10 Hz (30 Hz was used in the measurements).

3.2 Standing waves compensation method

A standing wave in the setup was suppressed by using the following technique. Two data points were taken with lambda over four separation in z-axis. These two points were added up with correction of the phase of Pi over two. The forward signal is then added constructively, unlike the first order reflections, which

has a phase difference of Pi. These reflections are added destructively. This method allows effectively suppress parasitic effects due to first order reflections for beams, close to a parallel. Band 9 receiver f#8 beam is close enough to achieve good standing wave suppression without degrading the quality of measurement itself. Additionally, an absorber plate around the source was used to decrease the level of reflections.

A small approx 2 x 1 mm flared waveguide probe was used as a radiation source. Its antenna beam is much wider than receiver f#8. No correction for source beam pattern is needed for analyzing results of measurements.

3.3 Room Temperature detector and saturation

An SLED (super lattice electronic device) [7] was mounted instead of an SIS junction in one of our mixer holder. That allows for using it mechanically with exactly the system which is going to be cooled down. This detector potentially has better conversion efficiency as conventional diode. Although, no specific matching circuit was designed to couple the SLED to an RF environment, signal to noise ratio of 72-80 dB has been obtained for all frequencies in ALMA band 9, using about 50-70 microwatt as an input signal. All measurements were done at room temperature. The SLED was pumped subharmonically. 36th harmonics of LO was typically used.

Since SLED is relatively new detector device for this type of measurements, a special attention was paid for detector saturation by the input signal. To check this effect, a measurements were done for the same beam of corrugated horn and scanning ranges while changing source output power. Results of this measurement are presented in fig. 6 and 7 for amplitude and phase respectively. No significant compression was found in the data as well as phase appears to be stable even for very significant drop (-33 dB) of input signal power.

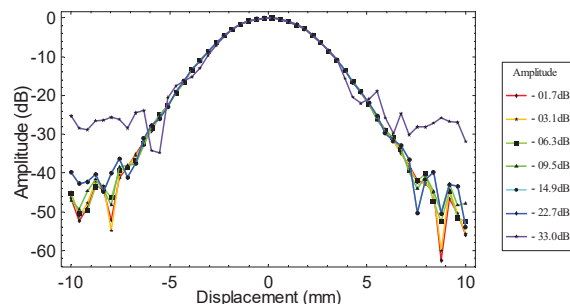


Fig. 6 Normalized amplitude field distribution measured at different signal source levels to check for a detector saturation effects.

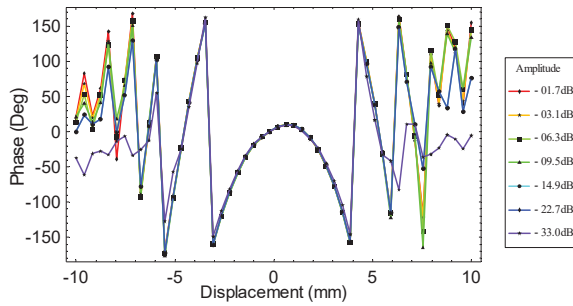


Fig. 7 Normalized phase field distribution measured at different signal source levels to check for detector saturation effects.

4. MEASUREMENT RESULTS

4.1 Laser beam propagation

The two-mirror block, presented in fig. 5 was produced by a CNC machining technique. Mirror surfaces were machined by a ball mill in the 5-axis CNC machine. After light polishing, the surface quality was good enough to put through a laser beam. The beam itself can be visualized by applying a water vapour fog during long time exposure of digital camera. The result is shown in fig. 8.

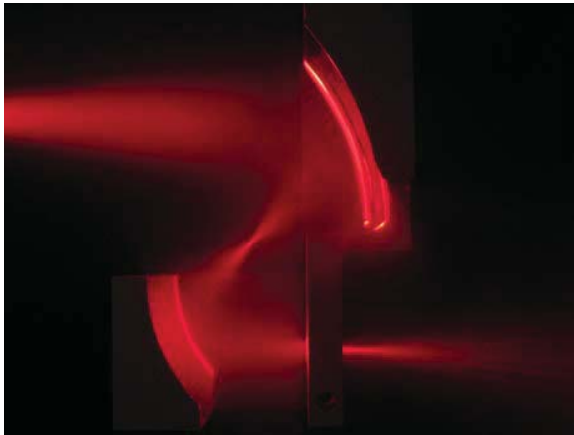


Fig. 8 Laser beam sent through machined two-mirror block.

Intermediate (tertiary focus) and final (quarterly focus) are clearly visible. Some beam splitting can be visible at lower right corner of the picture. This is due to approximation errors that occur during milling of the mirror surface. Note that frequency, at which the effect occurs, is 1000 times higher than the required frequency.

4.2 RF beam pattern measurement and analysis

A 2-D plot of amplitude and phase beam distributions are shown in fig. 9 and 10 respectively. The mirror

symmetrical axis coincide with Y-axis of scanner. One can see that a central maximum has a symmetrical shape both in phase and amplitude. A low levels of sidelobes is observed. A round ring structure at lower levels can be explained by periodical deviations of mirror shape from nominal curve due to machining strokes of the mill tool.

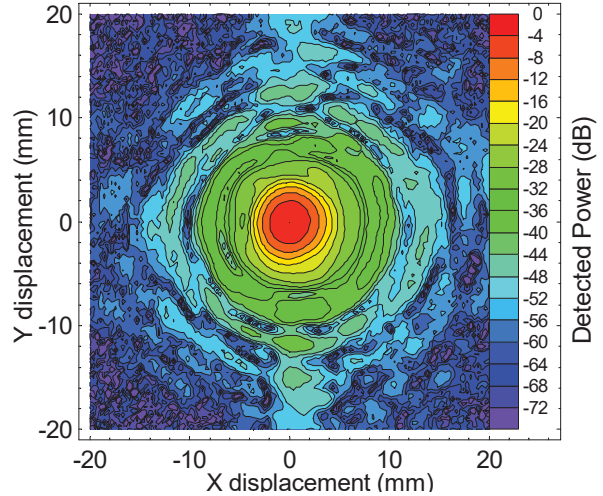


Fig. 9 Measured near field beam amplitude distribution of the two-mirror block at -50 mm from the waist plain. Frequency is 672 GHz.

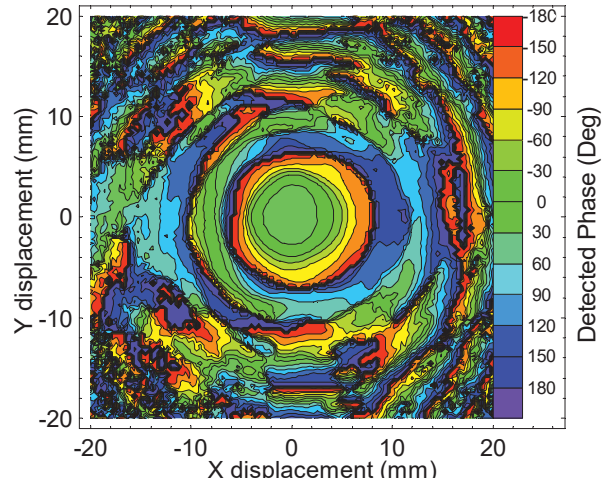


Fig. 10 Measured near field beam phase distribution of the two-mirror block at -50 mm from the waist plain. Frequency is 672 GHz.

Amplitude and phase information allows to calculate an overlap integral of the measured data with fundamental mode Gaussian beam. Ideally, this beam has six parameters, which can be determined from the data by maximizing Gaussian beam coupling: beam waist size, waist position (X,Y,Z), and two beam tilt angles. If the scanning plane is referenced to a mirror surface by a calibration device, obtained parameters allow to conclude if the production errors are still

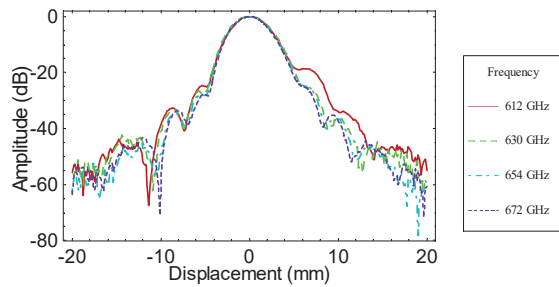


Fig. 11 Normalized amplitude field distribution measured along mirror asymmetrical axis at different signal frequencies.

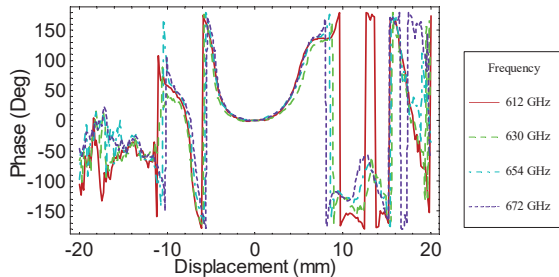


Fig. 12 Normalized phase field distribution measured along mirror asymmetrical axis at different signal frequencies.

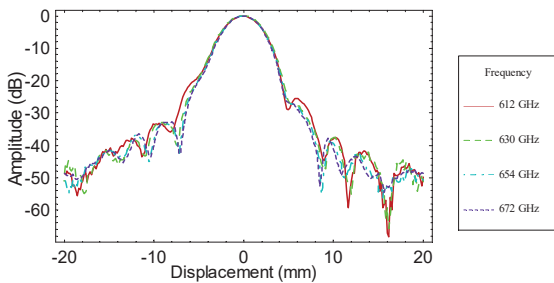


Fig. 13 Normalized amplitude field distribution measured along mirror symmetrical axis at different signal frequencies.

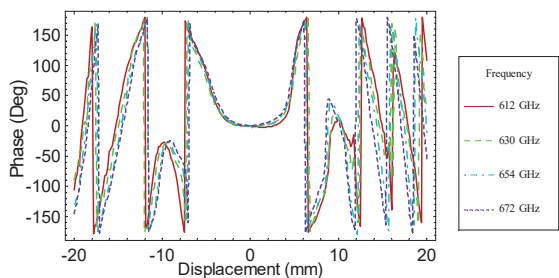


Fig. 14 Normalized phase field distribution measured along mirror asymmetrical axis at different signal frequencies.

acceptable and what the efficiency loss can be. The Gaussianness of the beam shown in fig. 9-10 is about 98%, which is very close to an ideal situation. The

waist size, offsets and tilt angle are within the required tolerances. It produces less than 1% efficiency loss, compared with an ideal case.

Measured beam cross-sections both for symmetrical (Y) and asymmetrical (X) mirror axes are shown in fig. 11-14. These measurements were done for several frequencies in ALMA band 9. Note that beam quality maintains over whole frequency range except the lowest frequency. At the lowest frequency, some deviation can be explained by a corrugated horn beam pattern change. A new horn design is underway.

As expected, the beam is largely symmetrical for symmetrical mirror axes. Visible operations effects are present in the cuts along the asymmetrical mirror axes. These effects, give rise to a beam tilt with respect to a nominal beam direction. Beam tilt, determined from measurements, is still within the required boundaries.

Finally, a far field antenna beam pattern can be determined from the 2-D data of fig. 9-10 by means of Fourier transform. The resulting amplitude angular distribution is shown in fig. 15 and central part of the distribution is shown in fig. 16 compared with the angular size of ALMA antenna secondary mirror. Since mirror is in the far field zone of the waist, this gives a good indication of the illumination edge taper. From fig. 16 one can conclude that the edge taper is very close to the required 12 dB and illumination pattern of the secondary is well centred. A semi-round fringes are visible at the beam pattern at very low signal levels. These fringes are again due to approximation error of the CNC machine (and due to tool movement stroke direction). However, still visible, these effects do not degrade significantly the illumination pattern at the secondary mirror.

Periodical mirror surface deviations produce a various peaks at far field pattern, see fig. 15. The angle of these peaks allows to determine the period of these deviations. Random deviations with white spectrum result in increase of a spill over from the main beam towards all directions uniformly. Good signal to noise level obtained in the figure and low level of peaks due to periodical deviations suggests that the selected production technique is sufficient for application in ALMA band 9 receiver.

5. CONCLUSION

An opto-mechanical layout of ALMA band 9 receiver is proposed. A production method of direct CNC machining of mirror surfaces and alignment of optics by assembly was demonstrated by building a prototype optics system and developing a near field beam pattern measurement system. The proposed technique proves

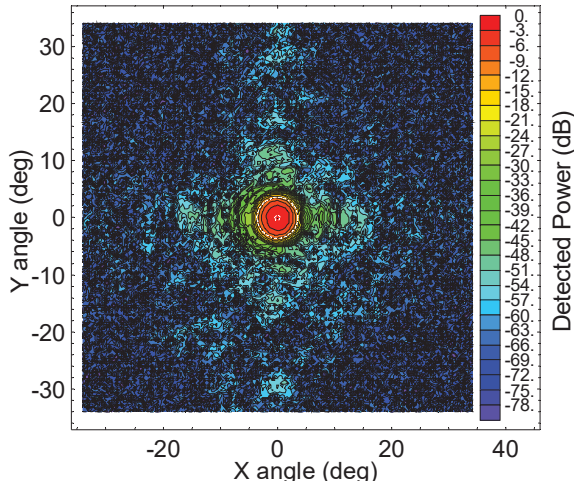


Fig. 15 Calculated far field amplitude angular distribution of the two-mirror block. Frequency is 672 GHz. The boundary of secondary mirror and central blockage of antenna are presented by a dashed line.

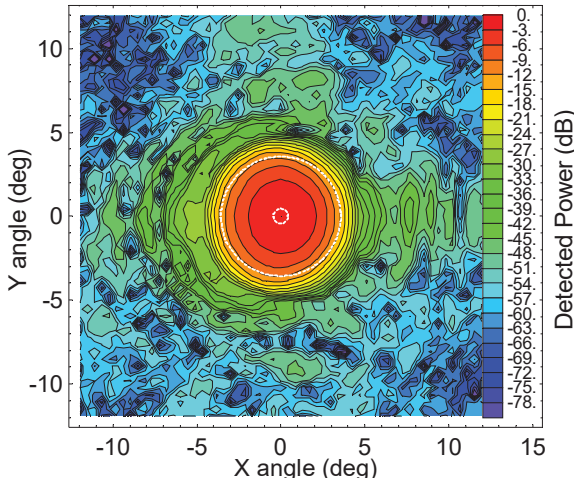


Fig. 16 Calculated far field amplitude angular distribution of the two-mirror block. Frequency is 672 GHz.

to be successful and can be applied for not only for ALMA band 9 but also for any ground based or space instrument requiring to build many copies of optics, for instance a free flying interferometer.

A super lattice electronic device (SLED) detector was successfully used as a replacement of an SIS junction for room temperature evaluation of optics layout. A signal to noise level as high as 80 dB has been achieved for 30 Hz detection bandwidth at 672 GHz signal frequency.

6. ACKNOWLEDGEMENT

The authors would like to thank Mark Harman of RAL for the overall design of the cartridges and cryostat that were given in section 1.2 We would also like to thank Fabrice Coq for the help in making the measurements. Authors also would like to thank Paveliev D.G. for providing SLED devices and Th. De Graauw for stimulating discussions.

7. REFERENCES

1. ALMA Receiver Optics Design, J.Lamb et al, ALMA memo 362
2. ALMA Project Book chapter 5, W.Wild et al.
3. ALMA Front-end Optics, M.Carter et al, to be published
4. ALMA Receiver Optics 2nd report, C-Y.Tham, S.Withington ALMA EDM
5. ALMA project Book, chapter 6 Cryogenics, A.Orlowska et al
6. Phase and Amplitude Measurements on an SIS Mixer fitted with a double slot Antenna for ALMA Band 9, M.Carter et al, Proceedings of The 13th International Symposium on Space Terahertz Technology
7. Schomburg et al, Electronics Letters, vol 35, No 17 (1999)